Fixed bed column study for the removal of Acid Blue 25 dye using NaOH-treated fallen leaves of *Ficus racemosa*

Suyog N. Jain, Parag R. Gogate*

*Chemical Engineering Department, Institute of Chemical Technology, Nathalal Parekh Marg, Matunga, Mumbai 400019, India,
Tel. +91 22 33612024; Fax: +91 22 33611020; emails: pr.gogate@ictmumbai.edu.in (P.R. Gogate), snjain@kkwagh.edu.in (S.N. Jain)*

ABSTRACT

The present study aims at evaluating the potential of adsorbent obtained from fallen leaves of *Ficus racemosa* with NaOH activation for Acid Blue 25 (AB 25) dye removal from aqueous solution in a continuous mode. The effect of various operating parameters such as bed height (2–6 cm), initial dye concentration (50–200 mg/L) and flow rate (6–10 mL/min) on the extent of dye removal has been investigated. The obtained results for the variation of operating parameters confirmed better column performance at higher bed height and lower flow rate. Different kinetic models such as Thomas, Adams–Bohart, Yoon–Nelson and bed depth service time (BDST) were applied to the obtained experimental data using column studies to predict the breakthrough curves and average mean square error has been employed to check the best suitability of the model. Thomas and BDST model predictions were established to be in better agreement with the experimental results. Maximum biosorption capacity for 100 mg/L of dye concentration present initially was obtained as 44.14 mg/g at optimum condition of 6 mL/min as the flow rate. The experimental observed capacity matched with the predicted biosorption capacity of 45.71 mg/g using the Thomas model. Elution studies conducted for seven cycles confirmed the reusability of synthesized biosorbent to treat industrial dye effluent in a column. Overall, the study clearly established the utility of synthesized biosorbent for the removal of AB 25 from wastewater in a continuous fixed bed adsorption process.

Keywords: Acid Blue 25; Sustainable biosorbent; Column study; Desorption; Kinetic models; *Ficus racemosa*

1. Introduction

In recent years, one of the serious environmental problems is the increasing pollution levels due to the presence of different toxic chemicals in the industrial effluents [1] that are refractory toward conventional approaches. One of the major effluents giving significant problems is the colored effluents released by textile industry [2] as it is the most difficult to treat [3] by the conventional approaches. The dye effluent contains different contaminants such as acid, base, color bearing dyes and toxic constituents [4]. Various sources discharging dye effluent to the water stream are textile finishing, dyestuff manufacturing, printing, ink, paper, leather and plastic industries [5,6]. Annual production of dyestuff is approximately 7×10^5 tones and 15% of the dyes produced are directly released into the effluents which may find their way into water bodies without suitable treatment [7]. Dyes are highly visible in water even at low concentration [8]. Dye effluents in water bodies can give rise to cancer, skin irritation and mutation [9] problems in humans on persistent exposure. Dyes give a blocking effect on the sunlight penetration affecting photosynthesis of aquatic plants and inhibit the growth of aquatic life [10]. Considering the adverse dye effluent effects on the environment, it is important to treat the dye effluents before discharging it into the water streams and hence development of the efficient dye removal methods is an important research area [11].

* Corresponding author.

Different physiochemical treatment methods have been applied by researchers for the dye removal from wastewater such as cloud point extraction [12], photocatalytic degradation [13,14], coagulation/flocculation [15], sonochemical degradation [16], membrane [17], electrochemical [18] and chemical oxidation [19]. However, these treatment techniques suffer from limitations of low removal efficiencies, complexity in operation and higher operating cost and hence are not considered to be effective to be applied for dye removal especially in the developing countries [20,21]. Adsorption offers a simple alternative for the removal of color from the wastewater and the advantages of adsorption compared with other techniques are flexibility, lower initial costs, ease of operation, simple design, insensitivity to toxic pollutants and applicability to treatment of wide range of compounds [4,22,23]. High quality treated effluent can be produced by suitably designed adsorption system [24,25]. In adsorption, activated carbon is widely used for dyes removal. However, it suffers from drawbacks of slow desorption kinetics, regeneration difficulties [26] and production of activated carbon is costlier process [27]. Hence, in recent years, research into development of efficient and cheaper adsorbents as an alternative to activated carbon is on forefront. Many of the biosorbents, in their natural form, such as *Citrus limetta* peel waste [28], natural zeolite tuff [29], coconut shell [30], garlic straw [31], longan shell [32], grapefruit peelings [33], oil palm leaves [34], *Ageratum conyzoides* leaf powder [35] and water hyacinth leaves [36] have been applied by investigators for dye removal. There have also been some reports related to the improvement in the adsorption capacity of the adsorbents using chemical activation and few examples of such modified biosorbents include surfactant-modified *Prunus dulcis* [37], Fe_3O_4-impregnated walnut shell [38], $FeCl_3$-activated *Rosa canina* L. leaves [39], $ZnCl_2$-activated corncob [40], NaClO- and NaOH-activated *Opuntia ficus-indica* fruit waste [41], HCl-activated montmorillonite [42], H_3PO_4-activated apricot stone [43] and H_2O_2-activated polyacrylonitrile fiber [44].

In our earlier work [45], a novel biosorbent was synthesized from *Ficus racemosa* (FR) fallen leaves with activation using NaOH and batch experiments were performed to determine the kinetic and thermodynamic parameters for the removal of Acid Blue 25 (AB 25) dye from wastewater. The work also established set of optimum parameters for maximum dye removal. The objective of present study is to investigate the potential of synthesized NaOH-treated FR (NTFR) biosorbent for the removal of AB 25 from wastewater in a continuous mode of operation, which is a very important study considering the possible commercial scale applications. The data obtained from batch experiments are typically not applicable for direct designs of the commercial scale operations due to the existence of insufficient contact time required to attain equilibrium. Hence, from the industrial treatment point of view, column adsorption studies at bench scale are important so as to establish the adaptability of continuous columns to versatile processes at commercial scale [46].

Fallen leaves of FR has been selected in the present study for the synthesis of adsorbent and subsequent application for dye removal in continuous column operation as it is a waste source, available in abundance and the utilization as adsorbent would also help in reducing waste biomass quantum.

A detailed literature survey also revealed that the application of fallen leaves of FR in a continuous mode of operation has not been explored for the removal of AB 25 and hence, the present study is novel in terms of exploring the use for removal of new dye. Using NaOH activation during the synthesis of adsorbent can help in increasing the surface area that can lead to significant biosorption capacity for AB 25 dye removal in continuous column and hence was applied in the present work for synthesis of efficient biosorbent. The regeneration study was also conducted in column to establish the potential of synthesized biosorbent for AB 25 dye removal in continuous reuse cycles. Such type of reusability studies in continuous operations have also not been reported in the literature for FR leaves–based biosorbent, which again confirms the novelty of the present work. AB 25 is selected as a model anthraquinonic dye in the present work due to its wide applications in industries such as ink, wool, nylon and paper [47]. The effects of bed height, initial dye concentration and flow rate on the extent of adsorption have been investigated. The entire research work in the present study has been performed at K. K. Wagh Institute of Engineering Education and Research, Nashik, Maharashtra, India

2. Materials and methods

2.1. Synthesis of biosorbent and characterization

Fallen leaves of FR were collected from Nashik, Maharashtra, India. The fallen leaves of FR, which has been selected as sustainable raw material, contain colored lignin that can create hurdle in measuring the color of dye solution and also the presence of lignin blocks the pores available on the adsorbent. Considering these aspects, NaOH treatment has been used for the removal of lignin. NaOH treatment involving impregnation of FR powder with NaOH followed by thermal treatment and subsequent distilled water washes was found to remove lignin from the powder. Synthesized NTFR biosorbent was kept in an airtight container before use in the column study. Detailed procedure for NTFR synthesis, characterization using different analytical methods, such as Scanning Electron Microscopy (SEM), Fourier Transform Infrared Spectroscopy (FTIR) and Brunauer–Emmett–Teller (BET), as well as the method for determination of pH corresponding to zero point charge (pH_{pzc}) have been explained in our earlier work [45].

2.2. Pollutant dye

AB 25 dye (molecular formula = $C_{20}H_{13}N_2NaO_5S$, molecular weight = 416.38 g/mol) was obtained from Sigma-Aldrich, Mumbai, as analytical grade dye, in the form of dark blue powder. The dye was used without any further treatment. Stock solution of 1,000 mg/L of AB 25 dye was prepared by dissolving 1 g of dye powder in 1 L of distilled water. The dye solutions of desired concentrations were subsequently prepared by dilution of the stock solution with distilled water.

2.3. Experimental methodology

All continuous operation adsorption experiments were conducted in a glass column of 2 cm internal diameter and 25 cm height. A layer of glass wool was packed at the top and bottom end of the column to avoid the adsorbent

loss and to ensure closely packed adsorbent arrangement. The packed biosorbent was also supported with the inert glass beads as shown in Fig. 1. The column experiments were conducted by pumping AB 25 dye solution in the upward direction with the help of variable speed peristaltic pump (Ravel Hiteks, Chennai, India). The experiments were performed at room temperature and the initial pH as 2. pH_{pzc} was obtained as 7.48. Hence, at lower pH (pH of 2) than pH_{pzc}, positive charge is developed on the biosorbent surface, which can yield maximum removal of anionic AB 25 dye. The effects of biosorbent bed height (2–4 cm), initial dye concentration (50–200 mg/L) and flow rate (6–10 mL/min) on the extent of dye removal have been investigated in the column mode of operation. The effluent dye samples were collected from the top of the adsorption column at different intervals of time and centrifuged in a research centrifuge (Remi Scientific, Mumbai) at speed of 8,000 rpm to remove any suspended particles. Supernatant samples were analyzed to determine AB 25 dye concentration (C_t) at λ_{max} of 602 nm using UV–visible spectrophotometer (UV 1800, Shimadzu, Japan). The obtained column data were fitted with various adsorption column models and model parameters were obtained to check the fitting of the model to the experimental results. Elution studies were also conducted for the set of experiments with initial dye concentration of 100 mg/L for seven cycles. All the column experiments were performed in triplicates and mean values were considered for further calculations.

2.4. Column data analysis

The performance of the adsorption column was analyzed with the help of breakthrough curve. The breakthrough curve was obtained by plotting the graph of C_t/C_i (where C_t is the concentration of dye at any time t, mg/L, and C_i is initial dye concentration, mg/L) vs. time. The breakthrough time (t_b) was determined as the time when dye concentration in the effluent reaches 10% of the initial concentration ($C_t/C_i = 0.1$) [48]. The exhaustion time (t_e) is determined as the time when dye concentration in the effluent reaches 90% of the initial concentration ($C_t/C_i = 0.9$) [49].
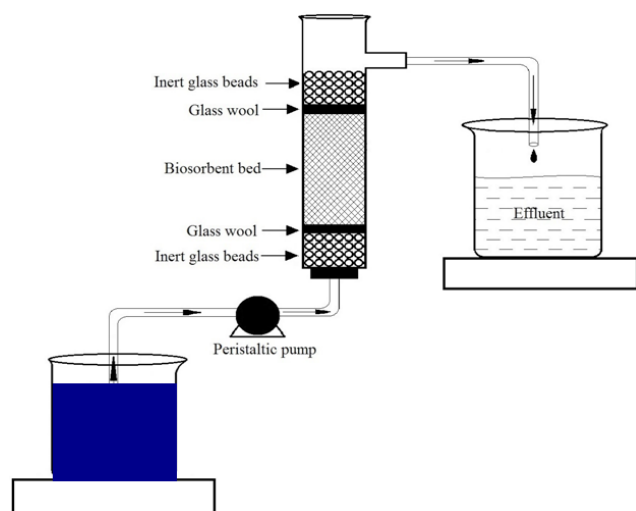

Fig. 1. Experimental setup of fixed bed column.

Effluent volume, V_{eff} (mL) processed in the operation is calculated as [27]:

$$V_{eff} = Qt_e \tag{1}$$

where Q is the volumetric flow rate of dye solution (mL/min) and t_e is the column exhaustion time (min).

Total dye adsorbed, q_{ad} (mg) for given dye concentration and flow rate is given as [50]:

$$q_{ad} = \frac{Q}{1000} \int_{t=0}^{t=t_{total}} C_{ad} dt \tag{2}$$

C_{ad} is the concentration of dye adsorbed on the biosorbent (mg/L) and t_{total} is total time of operation (min).

Dye adsorbed in milligrams per gram of biosorbent, q_{exp} (mg/g) was obtained as per the following equation [51]:

$$q_{exp} = \frac{q_{ad}}{m} \tag{3}$$

where m is mass of biosorbent in grams.

Similarly, uptake capacity at breakthrough (q_b, mg/g) has been calculated as [52]:

$$q_b = \frac{q_{ad,b}}{m} \tag{4}$$

where $q_{ad,b}$ is dye adsorbed (mg) at breakthrough.

Elution efficiency (E) has been determined as ratio of mass of dye desorbed from biosorbent (m_d) to mass of dye adsorbed on biosorbent (m_a) as per the following equation [53]:

$$E(\%) = \frac{m_d}{m_a} \times 100 \tag{5}$$

3. Results and discussion

3.1. Effect of bed height (H)

The effect of the bed height was investigated over the range of 2–6 cm considering the obtained results in the earlier work [44] related to batch adsorption giving the amount of adsorbent required for adequate separation and the quantum of adsorbent that could be effectively synthesized. Fig. 2 represents the obtained breakthrough curves at different bed heights of 2 cm (2.7 g of biosorbent), 4 cm (5.4 g) and 6 cm (8.1 g) at constant flow rate of 8 mL/min and initial dye concentration of 100 mg/L. As seen from Fig. 2, with a decrease in the bed height, the breakthrough curves become steeper indicating faster saturation, resulting in the early exhaustion of the bed [3]. The biosorption data were evaluated for the breakthrough parameters and obtained results have been given in Table 1. The slope of the breakthrough curve was found to decrease with an increase in the biosorbent bed height [54]. The breakthrough times and exhaustion times obtained in the present work increased from 50 to 210 min and from 225 to 720 min, respectively, with an increase in the bed height from 2 to 6 cm. In addition, for a similar increase in the bed height from 2 to 6 cm, maximum biosorption capacity increased from 35.68 ± 0.6 to 43.54 ± 0.77 mg/g. The increase in breakthrough and exhaustion times and biosorption capacity

can be attributed to the fact that more amount of biosorbent is available at higher bed heights which makes more sites available for the adsorption of dye molecules [2,55]. Similar trend has been reported for the removal of methylene blue using pinecone [56]. Considering the possible optimization of the quantity of adsorbent to be used, a bed height of 4 cm was considered for further studies.

3.2. Effect of initial dye concentration (C_i)

Fig. 3 depicts the obtained breakthrough curves at different initial dye concentrations of 50, 100 and 200 mg/L at a constant bed height of 4 cm and flow rate of 8 mL/min. Again the obtained results for the breakthrough parameters have been given in Table 1. The breakthrough time and exhaustion time decreased from 165 to 50 min and from 630 to 360 min, respectively, with an increase in dye concentration from 50 to 200 mg/L, which can be attributed to the early saturation of available adsorption sites at higher initial dye concentrations [57]. Similar trend has been reported for removal of methylene blue by activated carbon prepared from oil palm shell [58]. Treated effluent volume (Table 1) based on the experiments of continuous operation was also the lowest at the maximum dye concentration. The maximum biosorption capacity increased from 26.39 ± 0.26 to 52.40 ± 0.8 mg/g with

an increase in dye concentration from 50 to 200 mg/L, which can be attributed to the fact that driving force for the adsorption is based on the difference in dye quantity between the biosorbent surface and the remaining dye solution. Thus, with an increase in dye concentration, driving force for mass transfer increases which results in a corresponding increase in the biosorption capacity [23]. Considering the possible contradictory effects of higher adsorption capacity and lower volume of the effluent that could be treated, further experiments were performed using 100 mg/L as the initial concentration.

3.3. Effect of flow rate (Q)

Fig. 4 depicts the breakthrough curves at different dye flow rates of 6, 8 and 10 mL/min at a constant bed height of 4 cm and initial dye concentration of 100 mg/L. The breakthrough time and exhaustion time decreased from 165 to 80 min and from 750 to 330 min, respectively, with an increase in flow rate from 6 to 10 mL/min as per the data shown in Table 1. Increase in flow rate reduced the residence time of dye in the biosorbent bed and enhanced exposure of the new dye molecules in quick succession leading to early saturation of the bed and breakthrough was achieved quickly. Similar trend has been reported for removal of methylene blue using biosorbent based on oil palm empty fruit fibers [59] and for the removal of synthetic dyes from textile wastewater using immobilized
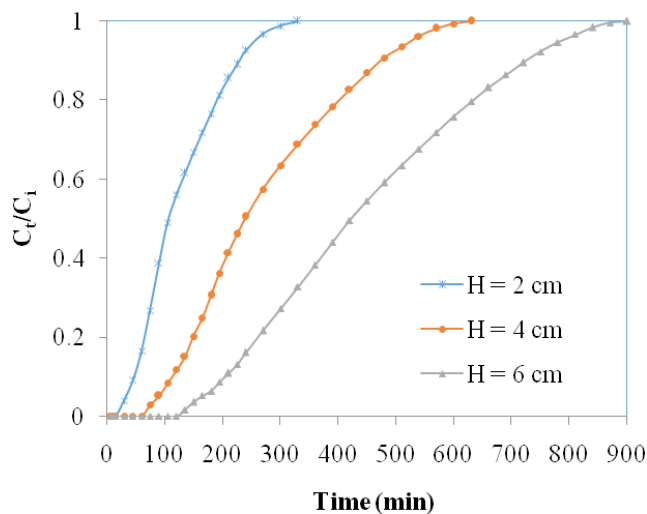

Fig. 2. Breakthrough curve for adsorption of AB 25 dye on NTFR biosorbent at different bed heights (pH$_i$ = 2, C_i = 100 mg/L, Q = 8 mL/min).
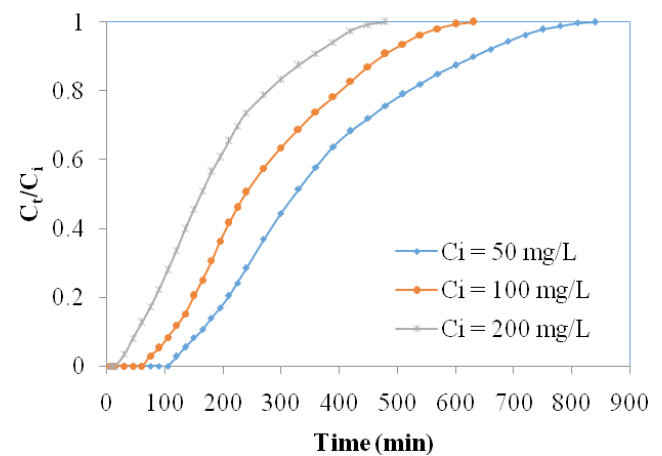

Fig. 3. Breakthrough curve for adsorption of AB 25 dye on NTFR biosorbent at different initial dye concentrations (pH$_i$ = 2, H = 4 cm, Q = 8 mL/min).

Table 1
Column data and breakthrough parameters at different bed height (H), initial dye concentration (C_i) and flow rate (Q)

H (cm)	C_i (mg/L)	Q (mL/min)	t_b (min)	$t_{0.5}$ (min)	t_e (min)	V_{eff} (L)	q_b (mg/g)	q_{exp} (mg/g)
2	100	8	50	105	225	1.8	11.47	35.68
4	100	8	120	240	480	3.84	14.54	39.28
6	100	8	210	420	720	5.76	19.79	43.54
4	50	8	165	330	630	5.04	11.61	26.39
4	200	8	50	165	360	2.88	15.51	52.40
4	100	6	165	360	750	4.5	17.43	44.14
4	100	10	80	180	330	3.3	12.59	34.74

dead *Candida tropicalis* [60]. The maximum biosorption capacity was found to decrease from 44.14 ± 0.79 to 34.74 ± 0.56 mg/g with an increase in the flow rate from 6 to 10 mL/min, which can be attributed to the steepening of the breakthrough curve with an increase in the flow rate. The increase in flow rate decreases residence time of dye and hence, the dye molecules do not get sufficient time to penetrate and diffuse into the biosorbent pores and dye leaves the bed before equilibrium is established resulting in decrease in biosorption capacity at high flow rates [46,61]. The observed results have clearly confirmed that efficient use of biosorbent is not favored at higher flow rates [52] and hence lower flow rates are recommended for better performance of the column in terms of complete utilization of the surface area and maximum adsorption.

3.4. Modeling of column data

The successful design of adsorption column requires development of good model which gives correct prediction of breakthrough curves for the removal of dye effluents. In the present study, different models for adsorption were applied for the breakthrough curve prediction. The different applied models in the present work and the obtained results for the fitting have been discussed below.

3.4.1. Thomas model

Thomas model [62] is often used for the prediction of adsorption column data and to study adsorption kinetics.
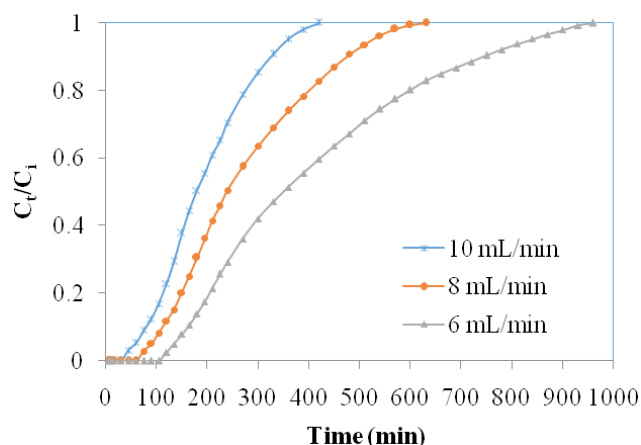

Fig. 4. Breakthrough curve for adsorption of AB 25 dye on NTFR biosorbent at different flow rates (pH$_i$ = 2, H = 4 cm, C_i = 100 mg/L).

This adsorption model fits the system especially when the internal and external diffusion resistances are very less. Thomas model assumes plug flow behavior in the column [63]. In addition, the model is based on the assumption that biosorption–desorption follows Langmuir kinetics without axial dispersion and the rate determining step follows second-order reversible kinetics [60]. The linearized form of the Thomas model has been given as follows:

$$\ln\left(\frac{C_i}{C_t} - 1\right) = \frac{k_{Th}q_{Th}m}{Q} - k_{Th}C_i t \tag{6}$$

where C_i and C_t are initial concentration and concentration of dye at any time t, respectively (mg/L), k_{Th} is Thomas rate constant (mL/min/mg), q_{Th} is maximum adsorption capacity (mg/g), m is mass of biosorbent (g), Q is flow rate (mL/min) and t is time (min).

The obtained experimental adsorption column data in terms of the adsorption capacity at different flow rate, height and concentration were fitted to the Thomas model for determination of Thomas parameters, the Thomas rate constant, k_{Th} and maximum adsorption capacity, q_{Th}. The obtained results for the linear fittings of Thomas model have been given in Table 2. As seen from Table 2, values of k_{Th} decreased and q_{Th} increased with an increase in bed height [64]. Increase in uptake (q_{Th}) can be attributed to increase in adsorption sites available due to more quantity of the adsorbent available at higher bed heights. Similar trend has been reported for removal of reactive azo dye onto granular activated carbon prepared from bamboo waste [63].

The observed values of k_{Th} decreased and q_{Th} increased with an increase initial dye concentration. Increase in concentration increased driving force for mass transfer and hence q_{Th} increased. Similar trend has been reported for removal of phenanthrene and acid red dye using modified kaolin [65]. Values of k_{Th} increased and q_{Th} decreased with an increase in flow rate. Retention time of dye in the column is less at high flow rate, which results in a decrease in the q_{Th}. Similar trend has been reported for removal of Acid Blue 15 using freshwater macroalga *Azolla filiculoides* [66] and removal of anionic blue 15 by using *Moringa oleifera*–encapsulated alginate beads [67]. From Table 2, it can be seen that the correlation coefficient, R^2 values range from 0.9534 to 0.9841, which are closer to unity. Maximum adsorption capacity values calculated experimentally, q_{exp} and obtained by Thomas model, q_{Th} were also observed to be very close to each other for all the set of parameters investigated in the work. These findings suggested better fitting of the Thomas model to the obtained experimental results.

Table 2
Thomas model parameters for removal of AB 25 by NTFR biosorbent

H (cm)	C_i (mg/L)	Q (mL/min)	k_{Th} (mL/min/mg)	q_{Th} (mg/g)	q_{exp} (mg/g)	R^2	MSE
2	100	8	0.244	37.59	35.68	0.9709	0.0027
4	100	8	0.13	40.21	39.28	0.9645	0.0026
6	100	8	0.097	44.29	43.54	0.9568	0.0017
4	50	8	0.206	27.08	26.39	0.9565	0.0022
4	200	8	0.0785	53.39	52.40	0.9653	0.0019
4	100	6	0.077	45.71	44.14	0.9534	0.0033
4	100	10	0.19	35.69	34.74	0.9841	0.0012

3.4.2. Adams–Bohart model

Adams–Bohart model [68] describes the variation in the C_t/C_i in a continuous adsorption process. This model assumes that rate of adsorption is proportional to residual adsorption capacity and concentration of the adsorbing species [64]. The linearized form of the Adams–Bohart model is given as follows:

$$\ln\left(\frac{C_t}{C_i}\right) = k_{AB}C_i t - k_{AB}N_0\frac{Z}{U} \tag{7}$$

where k_{AB} is Adams–Bohart rate constant (L/mg/min), N_0 is biosorption capacity of column (mg/L), U is velocity (cm/min) and Z is height of the biosorbent in the column (cm).

The obtained experimental adsorption column data were fitted to Adams–Bohart model for determination of the model parameters, Adams–Bohart rate constant, k_{AB} and biosorption capacity, N_0. The obtained results for the linear fittings of Adams–Bohart model have been given in Table 3. As seen from Table 3, values of N_0 increased and k_{AB} decreased with an increase in initial dye concentration and bed height whereas N_0 was found to decrease and k_{AB} found to increase with an increase in the flow rate. An increase in k_{AB} with an increase in the flow rate indicated that overall adsorption kinetics was dominated by external mass transfer in early stages of adsorption. Similar trend has been reported for removal of methylene blue by using polydopamine-coated silica microspheres [23]. It was observed in the present work (data shown in Table 3) that the correlation coefficient, R^2 values range from 0.7055 to 0.7905 which significantly deviate from unity. These findings suggest that the Adams–Bohart model does not fit very well the experimental results obtained in the present work.

3.4.3. Yoon–Nelson model

Yoon–Nelson model [69] is relatively a simple adsorption model describing breakthrough observed in the continuous column operation. The model assumes that the rate of decrease in the adsorption probability for each adsorbate molecule is proportional to the adsorbate–adsorption interaction probability and the adsorbate breakthrough probability [57]. The linearized form of the Yoon–Nelson model is given as follows:

$$\ln\left(\frac{C_t}{C_i - C_t}\right) = k_{YN}t - \tau k_{YN} \tag{8}$$

Simple rearrangement of the Eq. (8) gives the following new equation used for establishing the parameters:

$$\ln\left(\frac{C_i}{C_t} - 1\right) = -k_{YN}t + \tau k_{YN} \tag{9}$$

where k_{YN} is Yoon–Nelson rate constant (min^{-1}) and τ is the time required for 50% dye breakthrough (min) obtained from Yoon–Nelson model.

The obtained experimental adsorption column data were fitted to Yoon–Nelson model for the determination of Yoon–Nelson model parameters, Yoon–Nelson rate constant, k_{YN} and time required for 50% dye breakthrough, τ. The obtained results for the linear fittings of Yoon–Nelson model have been given in Table 4. It can be seen from Table 4 that k_{YN} increases and τ decreases with an increase in initial dye concentration. Increase in k_{YN} is due to increase in driving force for mass transfer at high concentrations and decrease in τ is due to faster saturation of the bed at higher concentration [70]. Similar trend has been reported for removal of

Table 3
Adams–Bohart model parameters for removal of AB 25 by NTFR biosorbent

H (cm)	C_i (mg/L)	Q (mL/min)	$k_{AB} \times 10^5$ (L/mg/min)	N_0 (mg/L)	R^2	MSE
2	100	8	9.6	29,635.91	0.7116	0.1813
4	100	8	5.2	30,561.35	0.7284	0.1040
6	100	8	4.3	30,586.30	0.7886	0.0890
4	50	8	7.8	20,646.84	0.7388	0.0939
4	200	8	3.1	43,995.54	0.7114	0.1292
4	100	6	3.1	35,866.77	0.7055	0.0706
4	100	10	8.8	24,900.46	0.7905	0.1709

Table 4
Yoon–Nelson model parameters for removal of AB 25 by NTFR biosorbent

H (cm)	C_i (mg/L)	Q (mL/min)	k_{YN} (min^{-1})	τ (min)	$t_{0.5}$ (min)	R^2	MSE
2	100	8	0.0244	126.86	105	0.9709	0.0027
4	100	8	0.013	271.39	240	0.9645	0.0026
6	100	8	0.0097	448.46	420	0.9568	0.0017
4	50	8	0.0103	365.58	330	0.9565	0.0022
4	200	8	0.0157	180.18	165	0.9653	0.0019
4	100	6	0.0077	411.38	360	0.9534	0.0033
4	100	10	0.019	192.73	180	0.9841	0.0012

Congo red dye using Romanian soil [53]. An increase in flow rate resulted in a corresponding increase in k_{YN} and decrease in τ. Similar trend has been reported for removal of ceph-alexin using the walnut shell–based activated carbon [71]. An increase in bed height resulted in a decrease in k_{YN} and increase in the τ, which can be attributed to slower saturation of the bed at higher bed heights [72]. Similar trend has been reported for removal of methylene blue dye using *Eucalyptus sheathiana* bark biomass [73]. From Table 4, it can be seen that the correlation coefficient, R^2 values range from 0.9534 to 0.9841, which are closer to unity. However, it was observed that the time required for 50% dye breakthrough calculated from model, τ and time required for 50% dye breakthrough obtained experimentally, $t_{0.5}$ were observed not to be very much closer to each other. These finding suggested fair fitting of the Yoon–Nelson model to the experimental results obtained in the present work.

3.4.4. Bed depth service time model

The bed depth service time (BDST) model [74] is a simple adsorption model that requires minimum column tests to determine necessary data. The model assumes that intra-particular diffusion forces and external resistance to mass transfer are negligible and surface reaction between the solute remaining in the solution and the unused adsorbent controls the adsorption kinetics [75]. The model establishes relationship between adsorbent bed height (Z) and operation time (t) in terms of process parameters. The linearized form of the BDST model is given as follows:

$$t = \frac{N_0 Z}{C_i U} - \frac{1}{k_a C_i} \ln\left(\frac{C_i}{C_t} - 1\right) \tag{10}$$

where N_0 is biosorption capacity of column (mg/L), U is linear velocity of solution through column (cm/min) and k_a is BDST rate constant (L/mg/min).

The obtained experimental adsorption column data were fitted to BDST model (Fig. 5) for determination of the model parameters, BDST rate constant, k_a and biosorption capacity of column, N_0. The obtained results for the linear fittings of

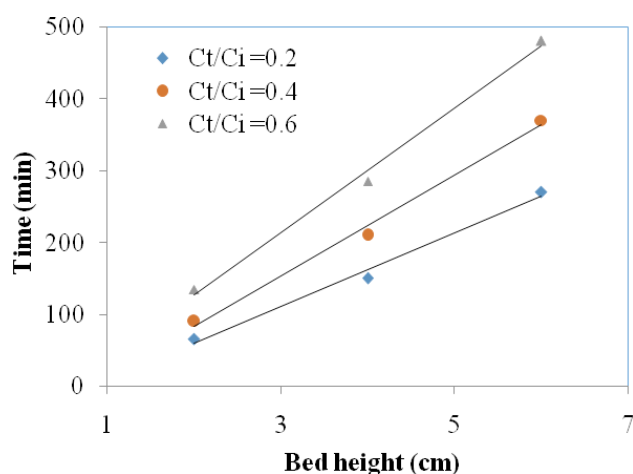Fig. 5. BDST model plot for adsorption of AB 25 dye on NTFR biosorbent ($pH_i = 2$, $Q = 8$ mL/min).

BDST model have been given in Table 5. It can be seen from Table 5 that N_0 increases and k_a decreases with an increase in C_t/C_i. The correlation coefficient, R^2 values range from 0.9904 to 0.9944, which are significantly closer to unity confirming the better fitting of the BDST model to the obtained experimental results. Similar trend has been reported for the removal of Congo red dye using rice husk–based biosorbent [76] and removal of Indosol Yellow BG dye using peanut husk–based biosorbent [77].

3.5. Comparison of the different models

In order to determine the best model to fit the experimental data obtained, it is necessary to analyze the column data using error analysis in addition to the observed values of the correlation coefficient. In the present study, average mean square error (MSE) has been employed to check the best suitability of the model [50]. The equation for the MSE calculation is as follows:

$$\text{MSE} = \frac{\sum\left[\left(\frac{C_t}{C_i}\right)_c - \left(\frac{C_t}{C_i}\right)_e\right]^2}{N} \tag{11}$$

where $(C_t/C_i)_c$ is the ratio of effluent to initial concentration of dye, calculated from model equations and $(C_t/C_i)_e$ is the ratio of effluent to initial concentration of dye, obtained experimentally. N is the number of experimental data points.

Linear regression has also been performed initially to determine all model parameters and correlation coefficient (R^2) values. Comparison of the obtained R^2 values for different models revealed that the values deviate significantly from unity for Adam–Bohart model as per the data shown in Table 3. On the other side, as seen from Table 2 and Table 4, R^2 values of Thomas and Yoon–Nelson model, respectively, are closer to unity. In addition, the R^2 values of BDST model (Table 5) are very close to unity also indicating better fitting of BDST model to the experimental data. In order to determine best fit among Thomas, Yoon–Nelson and Adams–Bohart models, breakthrough data obtained experimentally are compared with the predictions of the three models in Fig. 6. It can be seen from Fig. 6 that Thomas and Yoon–Nelson model values are close to experimental values whereas Adam–Bohart values are deviating from experimental values. These finding indicated that obtained experimental data do not fit to Adam–Bohart model. Graphs of Eq. 6 of Thomas model and Eq. 9 of Yoon–Nelson model are the same and represent a single curve, thus the correlation coefficient (R^2) and MSE values of these models are same for all studied parameters as seen from Tables 2 and 4. The least values of MSE were obtained for the Thomas and Yoon–Nelson model. The best fitting of

Table 5
BDST parameters for removal of AB 25 by NTFR biosorbent

C_t/C_i	N_0(mg/L)	$k_a \times 10^5$ (L/mg/min)	R^2
0.2	13,050.81	32	0.9904
0.4	17,825.50	7.2	0.9932
0.6	21,963.56	−9.01	0.9944

these two models to the obtained experimental results is also confirmed by comparing experimental values with the model values. However, it was observed that the Yoon–Nelson model parameter (τ) which is the time required for 50% dye breakthrough and the experimental value of time required for 50% dye breakthrough ($t_{0.5}$) are not very close to each other for all the studied parameters as seen from Table 4. On the other hand, the maximum adsorption capacity obtained by Thomas model (q_{Th}) and experimental value of the maximum adsorption capacity (q_{exp}) are very close to each other for all the studied parameters as seen from Table 2. All these findings suggest the best fitting of the Thomas model and comparatively fair fitness of Yoon–Nelson model to the experimental results.

3.6. Comparison of efficacy of adsorbent used in the present work with other biosorbents

In order to evaluate the potential of NTFR biosorbent to remove AB 25 dye from wastewater in continuous column, the maximum adsorption capacity (q_{exp}) obtained in the present study has been compared with adsorption capacity of some of the commonly reported adsorbents in the literature for the column operation for removal of different dyes (Table 6). It can be established from these data that NTFR biosorbent developed in the present study has comparatively good q_{exp} value, 44.14 mg/g. Hence, it is reasonable to suggest
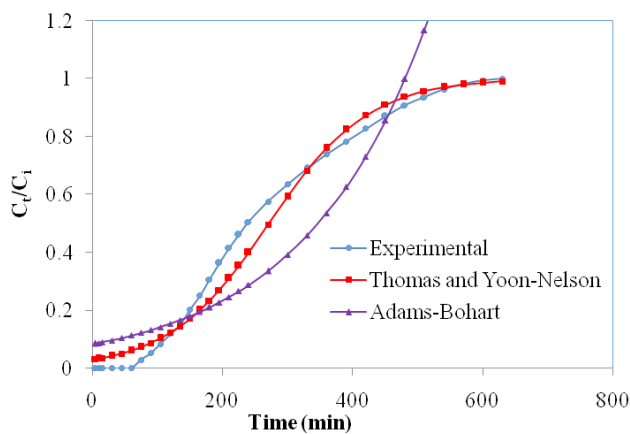

Fig. 6. Comparison of breakthrough curve (pH_i = 2, H = 4 cm, C_i = 100 mg/L, Q = 8 mL/min).

that NTFR biosorbent used in the present study is an efficient biosorbent to remove AB 25 from aqueous solution in continuous mode of operation.

3.7. Column regeneration studies

The economical viability of the adsorption process can be determined by regeneration of the biosorbent in a column and subsequent reuse for the adsorption. In the present study, column regeneration was performed based on the adsorption experiments using the AB 25 dye solution of 100 mg/L in the NTFR loaded column of 4 cm bed height at the rate of 8 mL/min, subsequent elution and reuse for seven cycles. NTFR biosorbent is regenerated in column by performing an elution step after each biosorption cycle. An elution step is based on the passage of distilled water under condition of pH of 12. AB 25 dye adsorption in column is carried out at lower pH (pH of 2) and elution is carried out at higher pH (pH of 12). High electrostatic attraction between acidic dye-loaded NTFR biosorbent and alkaline distilled water of pH 12 resulted in dye desorption at a faster rate. The elution efficiency values were found to be 99.93%, 99.06%, 97.76%, 96.07%, 94.57%, 90.96% and 85.71% from first to seven adsorption–elution cycles, respectively. Elution curve for seventh cycle in terms of the concentration of the dye in eluent after passage through the column is illustrated in Fig. 7. The obtained results for seven cycles established slight decrease in adsorption capacity from 39.28 mg/L for first cycle to 38.10 mg/g for fifth cycle, indicating excellent reusability of synthesized NTFR biosorbent to treat industrial dye effluent till five cycles. Subsequent increase in the reuse cycle resulted in a stronger decrease in the adsorption capacity (from 38.1 mg/g in the fifth cycle to 36.02 mg/g in the seventh cycle). It is important to understand that almost 90% of dye removal always occurred in less than 30 min for all cycles. The obtained results for seven cycles indicated that synthesized NTFR biosorbent in the present study could be regenerated in a column and used repeatedly for dye removal from aqueous solution with minimal loss in the adsorption capacity till five cycles and with marginally reduced capacities for seven cycles. The presented regeneration results ensured potential of synthesized biosorbent to treat textile dye effluents at larger scale and more importantly in continuous mode of operation.

Table 6
Comparison of column maximum adsorption capacity (q_{exp}) of different adsorbents with NTFR

| Dye	Adsorbent	C_i (mg/L)	Flow rate (mL/min)	Column height (cm)	q_{exp} (mg/g)	References
AB 25	NTFR	100	6	4	44.14	Present study
Direct Yellow 50	Sugarcane bagasse	50	1.8	4	10.44	[2]
Reactive Black 5	Bamboo waste	100	10	8	39.02	[63]
Congo red	Rice husk	30	3.6	12	3.08	[76]
Indosol Yellow BG	Peanut husk	100	1.8	4	25.92	[77]
Methylene blue	Natural zeolite	30	2.2	15	4.36	[78]
Methylene blue	Modified chitin supported on sand	50	10	15	51.8	[79]
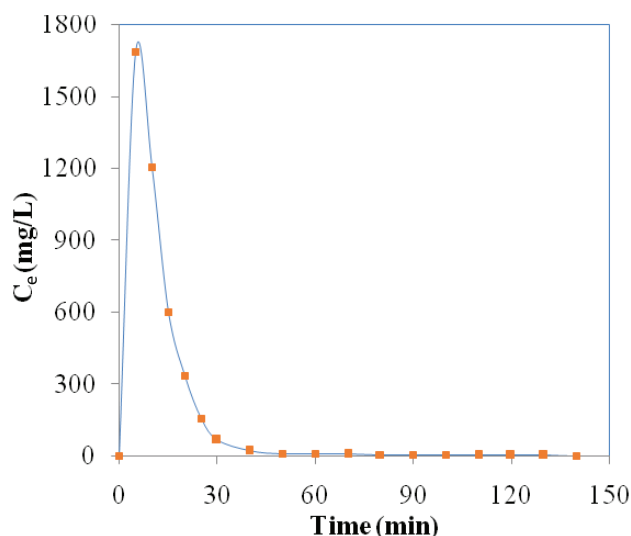
Fig. 7. Elution curve for seventh cycle for adsorption of AB 25 dye on NTFR biosorbent (pH$_i$ = 2, H = 4 cm C_i = 100 mg/L, Q = 8 mL/min).

4. Conclusions

The present study established the potential of synthesized NTFR biosorbent for the removal of AB 25 from aqueous solution in a continuous mode of operation. The established breakthrough curves represented the effect of biosorbent bed height, initial dye concentration and flow rate on AB 25 dye removal in a fixed bed column. Higher bed height (6 cm) and lower flow rate (6 mL/min) favored maximum AB 25 dye removal from aqueous solution. The maximum biosorption capacity for 100 mg/L of dye concentration was observed to be 44.14 mg/g. Thomson and BDST model were found to provide the best fit to the column experimental data as per the values of the correlation coefficient as well as the error function, MSE. Elution studies conducted for seven cycles established slight decrease in adsorption capacity from 39.28 mg/L for first cycle of reuse to 38.10 mg/g for fifth cycle, indicating potential reusability of synthesized NTFR biosorbent to treat industrial dye effluent, whereas adsorption capacity marginally decreased from 38.1 mg/g in the fifth cycle to 36.02 mg/g in the seventh cycle. Overall, it has been established that the NTFR biosorbent serves as a low cost biosorbent and can be considered as promising biosorbent for removal of AB 25 dye from wastewater in a continuous mode of operation based on the fixed bed.

Acknowledgments

References

[1] W. Zhang, H. Yan, H. Li, Z. Jiang, L. Dong, X. Kan, H. Yang, A. Li, R. Cheng, Removal of dyes from aqueous solutions by straw based adsorbents: batch and column studies, Chem. Eng. J., 168 (2011) 1120–1127.

[2] S. Sadaf, H. Nawaz, S. Nausheen, M. Amin, Application of a novel lignocellulosic biomaterial for the removal of Direct Yellow 50 dye from aqueous solution: batch and column study, J. Taiwan Inst. Chem. Eng., 47 (2015) 160–170.

[3] O. Ozdemir, M. Turan, A.Z. Turan, A. Faki, A.B. Engin, Feasibility analysis of color removal from textile dyeing wastewater in a fixed-bed column system by surfactant-modified zeolite (SMZ), J. Hazard. Mater., 166 (2009) 647–654.

[4] V.K. Gupta, S.K. Srivastava, D. Mohan, Equilibrium uptake, sorption dynamics, process optimization, and column operations for the removal and recovery of malachite green from wastewater using activated carbon and activated slag, Ind. Eng. Chem. Res., 36 (1997) 2207–2218.

[5] A. Goshadrou, A. Moheb, Continuous fixed bed adsorption of C.I. Acid Blue 92 by exfoliated graphite: an experimental and modeling study, Desalination, 269 (2011) 170–176.

[6] M. Hadi, M.R. Samarghandi, G. Mckay, Simplified fixed bed design models for the adsorption of acid dyes on novel pine cone derived activated carbon, Water Air Soil Pollut., 218 (2011) 197–212.

[7] K. Jung, B.H. Choi, M. Hwang, T. Jeong, K. Ahn, Fabrication of granular activated carbons derived from spent coffee grounds by entrapment in calcium alginate beads for adsorption of acid orange 7 and methylene blue, Bioresour. Technol., 219 (2016) 185–195.

[8] T.M. Albayati, A.A. Sabri, R.A. Alazawi, Separation of Methylene Blue as pollutant of water by SBA-15 in a fixed-bed column, Arab. J. Sci. Eng., 41 (2016) 2409–2415.

[9] N. Sivarajasekar, R. Baskar, Biosorption of basic violet 10 onto activated *Gossypium hirsutum* seeds: batch and fixed-bed column studies, Chinese J. Chem. Eng., 23 (2015) 1610–1619.

[10] M. Saeed, R. Nadeem, M. Yousaf, Removal of industrial pollutant (Reactive Orange 122 dye) using environment-friendly sorbent *Trapa bispinosa*'s peel and fruit, Int. J. Environ. Sci. Technol., 12 (2015) 1223–1234.

[11] K.S. Bharathi, S.T. Ramesh, Removal of dyes using agricultural waste as low-cost adsorbents: a review, Appl. Water Sci., 3 (2013) 773–790.

[12] D.R. Bhatt, K.C. Maheria, J.K. Parikh, Determination of thermodynamics and design parameters for ionic liquid-induced cloud point extraction of Coralene red dye, Int. J. Environ. Sci. Technol., 13 (2016) 589–598.

[13] A. Ajmal, I. Majeed, R.N. Malik, M. Iqbal, M.A. Nadeem, I. Hussain, S. Yousuf, G. Mustafa, M.I. Zafar, M.A. Nadeem, Photocatalytic degradation of textile dyes on Cu_2O-CuO/TiO_2 anatase powders, J. Environ. Chem. Eng., 4 (2016) 2138–2146.

[14] K. Tanaka, K. Padermpole, T. Hisanaga, Photocatalytic degradation of commercial azo dyes, Water Res., 34 (2000) 327–333.

[15] M. Khayet, A.Y. Zahrim, N. Hilal, Modelling and optimization of coagulation of highly concentrated industrial grade leather dye by response surface methodology, Chem. Eng. J., 167 (2011) 77–83.

[16] S. Dalhatou, C. Petrier, S. Laminsi, S. Baup, Sonochemical removal of naphthol blue black azo dye: influence of parameters and effect of mineral ions, Int. J. Environ. Sci. Technol., 12 (2015) 35–44.

[17] M.R.S. Kebria, M. Jahanshahi, A. Rahimpour, SiO_2 modified polyethyleneimine-based nano filtration membranes for dye removal from aqueous and organic solutions, Desalination, 367 (2015) 255–264.

[18] V.S.K. Yadav, M.K. Purkait, Simultaneous CO_2 reduction and dye (crystal violet) removal electrochemically on Sn and Zn electrocatalysts using Co_3O_4 anode, Energy Fuels, 30 (2016) 3340–3346.

[19] I.A. Salem, Activation of H_2O_2 by Amberlyst-15 resin supported with copper(II)-complexes towards oxidation of crystal violet, Chemosphere, 44 (2001) 1109–1119.

[20] A. Adak, M. Bandyopadhyay, A. Pal, Fixed bed column study for the removal of crystal violet (C. I. Basic Violet 3) dye from aquatic environment by surfactant-modified alumina, Dye Pigm., 69 (2006) 245–251.

[21] H.I. Albroomi, M.A. Elsayed, A. Baraka, M.A. Abdelmaged, Batch and fixed-bed adsorption of tartrazine azo-dye onto activated carbon prepared from apricot stones, Appl. Water Sci., 7 (2017) 2063–2074.

[22] G. Crini, Kinetic and equilibrium studies on the removal of cationic dyes from aqueous solution by adsorption onto a cyclodextrin polymer, Dye Pigm., 77 (2008) 415–426.

[23] T.A. Germi, A. Nematollahzadeh, Bimodal porous silica microspheres decorated with polydopamine nanoparticles for the adsorption of methylene blue in fixed-bed columns, J. Colloid Interface Sci., 470 (2016) 172–182.

[24] G. Crini, Non-conventional low-cost adsorbents for dye removal: a review, Bioresour. Technol., 97 (2006) 1061–1085.

[25] S.E. Subramani, N. Thinakaran, Isotherm, kinetic and thermodynamic studies on the adsorption behavior of textile dyes onto chitosan, Process Saf. Environ. Prot., 106 (2016) 1–10.

[26] P. Liao, Z. Zhan, J. Dai, X. Wu, W. Zhang, K. Wang, S. Yuan, Adsorption of tetracycline and chloramphenicol in aqueous solutions by bamboo charcoal: a batch and fixed-bed column study, Chem. Eng. J., 228 (2013) 496–505.

[27] R. Aravindhan, J.R. Rao, B.U. Nair, Preparation and characterization of activated carbon from marine macro-algal biomass, J. Hazard. Mater., 162 (2009) 688–694.

[28] S. Shakoor, A. Nasar, Removal of methylene blue dye from artificially contaminated water using *Citrus limetta* peel waste as a very low cost adsorbent, J. Taiwan Inst. Chem. Eng., 66 (2016) 154–163.

[29] I. Humelnicu, A. Baiceanu, M. Ignat, V. Dulman, The removal of Basic Blue 41 textile dye from aqueous solution by adsorption onto natural zeolitic tuff: kinetics and thermodynamics, Process Saf. Environ. Prot., 105 (2017) 274–287.

[30] A. Umar Isha, G. Abdulraheem, S. Bala, S. Muhammad, M. Abdullahi, Kinetics, equilibrium and thermodynamics studies of C.I. Reactive Blue 19 dye adsorption on coconut shell based activated carbon, Int. Biodeterior. Biodegradation, 102 (2015) 265–273.

[31] F. Kallel, F. Chaari, F. Bouaziz, F. Bettaieb, R. Ghorbel, S.E. Chaabouni, Sorption and desorption characteristics for the removal of a toxic dye, methylene blue from aqueous solution by a low cost agricultural by-product, J. Mol. Liq., 219 (2016) 279–288.

[32] Y. Wang, L. Zhu, H. Jiang, F. Hu, X. Shen, Application of longan shell as non-conventional low-cost adsorbent for the removal of cationic dye from aqueous solution, Spectrochim. Acta., 159 (2016) 254–261.

[33] E. Rosales, J. Meijide, T. Tavares, M. Pazos, M.A. Sanromán, Grapefruit peelings as a promising biosorbent for the removal of leather dyes and hexavalent chromium, Process Saf. Environ. Prot., 101 (2016) 61–71.

[34] H.D. Setiabudi, R. Jusoh, S.F.R.M. Suhaimi, S.F. Masrur, Adsorption of methylene blue onto oil palm (*Elaeis guineensis*) leaves: process optimization, isotherm, kinetics and thermodynamic studies, J. Taiwan Inst. Chem. Eng., 63 (2016) 363–370.

[35] E.H. Ezechi, S.R. bin Mohanmed Kutty, A. Malakahmad, M.H. Isa, Characterization and optimization of effluent dye removal using a new low cost adsorbent: equilibrium, kinetics and thermodynamic study, Process Saf. Environ. Prot., 98 (2015) 16–32.

[36] I. Guerrero-coronilla, L. Morales-barrera, E. Cristiani-urbina, Kinetic, isotherm and thermodynamic studies of amaranth dye biosorption from aqueous solution onto water hyacinth leaves, J. Environ. Manage., 152 (2015) 99–108.

[37] S.N. Jain, P.R. Gogate, Acid Blue 113 removal from aqueous solution using novel biosorbent based on NaOH treated and surfactant modified fallen leaves of *Prunus dulcis*, J. Environ. Chem. Eng., 5 (2017) 3384–3394.

[38] M. Ashrafi, M.A. Chamjangali, G. Bagherian, N. Goudarzi, Application of linear and non-linear methods for modeling removal efficiency of textile dyes from aqueous solutions using magnetic Fe_3O_4 impregnated onto walnut shell, Spectrochim. Acta., 171 (2016) 268–279.

[39] S. Agarwal, I. Tyagi, V.K. Gupta, S. Mashhadi, M. Ghasemi, Kinetics and thermodynamics of Malachite Green dye removal from aqueous phase using iron nanoparticles loaded on ash, J. Mol. Liq., 223 (2016) 1340–1347.

[40] H. Ma, J. Li, W. Liu, M. Miao, B. Cheng, S. Zhu, Novel synthesis of a versatile magnetic adsorbent derived from corncob for dye removal, Bioresour. Technol., 190 (2015) 13–20.

[41] A.A. Peláez-cid, I. Velázquez-ugalde, A.M. Herrera-gonzález, J. García-serrano, Textile dyes removal from aqueous solution using *Opuntia ficus-indica* fruit waste as adsorbent and its characterization, J. Environ. Manage., 130 (2013) 90–97.

[42] M.-Y. Teng, S.-H. Lin, Removal of basic dye from water onto pristine and HCl-activated montmorillonite in fixed beds, Desalination, 194 (2006) 156–165.

[43] M. Abbas, M. Trari, Kinetic, equilibrium and thermodynamic study on the removal of Congo red from aqueous solutions by adsorption onto apricot stone, Process Saf. Environ. Prot., 98 (2015) 424–436.

[44] Z. Han, X. Han, X. Zhao, J. Yu, H. Xu, Iron phthalocyanine supported on amidoximated PAN fiber as effective catalyst for controllable hydrogen peroxide activation in oxidizing organic dyes, J. Hazard. Mater., 320 (2016) 27–35.

[45] S.N. Jain, P.R. Gogate, NaOH-treated dead leaves of *Ficus racemosa* as an efficient biosorbent for Acid Blue 25 removal, Int. J. Environ. Sci. Technol., 14 (2017) 531–542.

[46] M.T. Uddin, M. Rukanuzzaman, M.M.R. Khan, M.A. Islam, Adsorption of methylene blue from aqueous solution by jackfruit (*Artocarpus heteropyllus*) leaf powder: a fixed-bed column study, J. Environ. Manage., 90 (2009) 3443–3450.

[47] O. Duman, S. Tunç, B. Kancı, Spectrophotometric studies on the interactions of C.I. Basic Red 9 and C.I. Acid Blue 25 with hexadecyltrimethylammonium bromide in cationic surfactant micelles, Fluid Phase Equilib., 301 (2011) 56–61.

[48] A. Faki, M. Turan, O. Ozdemir, A.Z. Turan, Analysis of fixed-bed column adsorption of reactive yellow 176 onto surfactant-modified zeolite, Ind. Eng. Chem. Res., 47 (2008) 6999–7004.

[49] S. Netpradit, P. Thiravetyan, S. Towprayoon, Evaluation of metal hydroxide sludge for reactive dye adsorption in a fixed-bed column system, Water Res. 38 (2004) 71–78.

[50] L. Cavas, Z. Karabay, H. Alyuruk, H. Dogan, G.K. Demir, Thomas and artificial neural network models for the fixed-bed adsorption of methylene blue by a beach waste *Posidonia oceanica* (L.) dead leaves, Chem. Eng. J., 171 (2011) 557–562.

[51] M. Foroughi-dahr, M. Esmaieli, H. Abolghasemi, A. Shojamoradi, E.S. Pouya, Continuous adsorption study of Congo red using tea waste in a fixed-bed column, Desal. Wat. Treat., 57 (2015) 8437–8446.

[52] A. Chatterjee, S. Schiewer, Biosorption of cadmium (II) ions by citrus peels in a packed bed column: effect of process parameters and comparison of different breakthrough curve models, Clean Soil Air Water, 39 (2011) 874–881.

[53] C. Smaranda, M. Popescu, D. Bulgariu, T. Măluțan, M. Gavrilescu, Adsorption of organic pollutants onto a Romanian soil: column dynamics and transport, Process Saf. Environ. Prot., 108 (2017) 108–120.

[54] B. Zhao, Y. Shang, W. Xiao, C. Dou, R. Han, Adsorption of Congo red from solution using cationic surfactant modified wheat straw in column model, J. Environ. Chem. Eng., 2 (2014) 40–45.

[55] J. Barron-zambrano, A. Szygula, M. Ruiz, A.M. Sastre, E. Guibal, Biosorption of Reactive Black 5 from aqueous solutions by chitosan: column studies, J. Environ. Manage., 91 (2010) 2669–2675.

[56] M.T. Yagub, T.K. Sen, S. Afroze, H.M. Ang, Fixed-bed dynamic column adsorption study of methylene blue (MB) onto pine cone, Desal. Wat. Treat., 55 (2015) 1026–1039.

[57] Z. Aksu, F. Gönen, Biosorption of phenol by immobilized activated sludge in a continuous packed bed: prediction of breakthrough curves, Process Biochem., 39 (2004) 599–613.

[58] I.A.W. Tan, A.L. Ahmad, B.H. Hameed, Adsorption of basic dye using activated carbon prepared from oil palm shell: batch and fixed bed studies, Desalination, 225 (2008) 13–28.

[59] M.S. Sajab, C.H. Chia, S. Zakaria, M. Sillanpää, Fixed-bed column studies for the removal of cationic and anionic dyes by chemically modified oil palm empty fruit bunch fibers: single- and multi-solute systems, Desal. Wat. Treat., 55 (2015) 1372–1379.

[60] D. Charumathi, N. Das, Packed bed column studies for the removal of synthetic dyes from textile wastewater using immobilised dead *C. tropicalis*, Desalination, 285 (2012) 22–30.

[61] M. Karimi, A. Shojaei, A. Nematollahzadeh, M.J. Abdekhodaie, Column study of Cr (VI) adsorption onto modified silica – polyacrylamide microspheres composite, Chem. Eng. J., 210 (2012) 280–288.

[62] H.C. Thomas, Heterogeneous ion exchange in a flowing system, J. Am. Chem. Soc., 66 (1944) 1664–1666.

[63] A.A. Ahmad, B.H. Hameed, Fixed-bed adsorption of reactive azo dye onto granular activated carbon prepared from waste, J. Hazard. Mater., 175 (2010) 298–303.

[64] R. Han, Y. Wang, X. Zhao, Y. Wang, F. Xie, J. Cheng, M. Tang, Adsorption of methylene blue by phoenix tree leaf powder in a fixed-bed column: experiments and prediction of breakthrough curves, Desalination, 245 (2009) 284–297.

[65] I.A. Lawal, B. Moodleya, Column, kinetic and isotherm studies of PAH (phenanthrene) and dye (acid red) on kaolin modified with 1-hexyl, 3-decahexyl imidazolium ionic liquid, J. Environ. Chem. Eng., 4 (2016) 2774–2784.

[66] T.V.N. Padmesh, K. Vijayaraghavan, G. Sekaran, M. Velan, Biosorption of Acid Blue 15 using fresh water macroalga *Azolla filiculoides*: batch and column studies, Dye Pigm., 71 (2006) 77–82.

[67] R. Kannan, S. Lakshmi, N. Aparna, S. Prabhakar, W.R. Thilagaraj, Eco-friendly treatment of textile dye from aqueous solution using encapsulated biosorbent matrix beads: kinetics and breakthrough analysis, Int. J. Ind. Chem., 7 (2016) 265–275.

[68] Ç. Sarici-Özdemir, Removal of Methylene Blue by activated carbon prepared from waste in a fixed-bed column, Part. Sci. Technol., 32 (2014) 311–318.

[69] Y.H. Yoon, J.H. Nelson, Application of gas adsorption kinetics I. A theoretical model for respirator cartridge service life, Am. Ind. Hyg. Assoc. J., 45 (1984) 509–516.

[70] K.Z. Setshedi, M. Bhaumik, M.S. Onyango, A. Maity, Breakthrough studies for Cr(VI) sorption from aqueous solution using exfoliated polypyrrole-organically modified montmorillonite clay nanocomposite, J. Ind. Eng. Chem., 20 (2014) 2208–2216.

[71] G. Nazari, H. Abolghasemi, M. Esmaieli, E.S. Pouya, Aqueous phase adsorption of cephalexin by walnut shell-based activated carbon: a fixed-bed column study, Appl. Surf. Sci., 375 (2016) 144–153.

[72] N. Rahman, M.F. Khan, Nitrate removal using poly-o-toluidine zirconium (IV) ethylenediamine as adsorbent: batch and fixed-bed column adsorption modelling, J. Water Process Eng., 9 (2016) 254–266.

[73] S. Afroze, T.K. Sen, H.M. Ang, Adsorption performance of continuous fixed bed column for the removal of methylene blue (MB) dye using *Eucalyptus sheathiana* bark biomass, Res. Chem. Intermed., 42 (2016) 2343–2364.

[74] R.A. Hutchins, New method simplifies design of activated carbon systems, Chem. Eng., 80 (1973) 133–138.

[75] S.S. Baral, N. Das, T.S. Ramulu, S.K. Sahoo, S.N. Das, G.R. Chaudhury, Removal of Cr(VI) by thermally activated weed *Salvinia cucullata* in a fixed-bed column, J. Hazard. Mater., 161 (2009) 1427–1435.

[76] R. Han, D. Ding, Y. Xu, W. Zou, Y. Wang, Y. Li, L. Zou, Use of rice husk for the adsorption of Congo red from aqueous solution in column mode, Bioresour. Technol., 99 (2008) 2938–2946.

[77] S. Sadaf, H.N. Bhatti, Batch and fixed bed column studies for the removal of Indosol Yellow BG dye by peanut husk, J. Taiwan Inst. Chem. Eng., 45 (2014) 541–553.

[78] R. Han, Y. Wang, W. Zou, Y. Wang, J. Shi, Comparison of linear and nonlinear analysis in estimating the Thomas model parameters for methylene blue adsorption onto natural zeolite in fixed-bed column, J. Hazard. Mater., 145 (2007) 331–335.

[79] G.L. Dotto, J.M.N. dos Santos, R. Rosa, L.A.A. Pinto, F.A. Pavan, E.C. Lima, Fixed bed adsorption of Methylene Blue by ultrasonic surface modified chitin supported on sand, Chem. Eng. Res. Des., 100 (2015) 302–310.